2nd International Conference on Sensing Technology
November 26-28, 2007 Palmerston North, New Zealand

SAW Parameter Extraction Using Finite Element Analysis

Ajay Tikka[1] Said Al-Sarawi[1] and Derek Abbott[2]
[1]The Centre for High Performance Integrated Technologies and Systems (CHiPTec),
[2]Centre for Biomedical Engineering,
The University of Adelaide, SA 5005, Australia.
ajay.tikka@adelaide.edu.au, alsarawi@eleceng.adelaide.edu.au, dabbott@eleceng.adelaide.edu.au

Abstract

Surface acoustic wave devices apart from being small, rugged and reliable can also be used as wirelessly interrogatable and completely passive devices in hostile environments. As complex signal processing functions can be performed with a simple structure through the variation of electrode patterns they can power wireless sensors and actuators in a secure manner. It is important to develop exact SAW parameter measurement techniques and simulation methods that are able to model the SAW devices accurately. Contrary to the frequently used FEM/BEM numerical simulation techniques, in this paper a versatile finite element modelling is employed to automatically include the second order effects in the device by considering the complete set of partial differential equations. The eigenmodes and the harmonic admittance of a periodic structure obtained from the FEM simulations are used to extract the COM/P-matrix parameters with the help of a fitting technique. The extracted parameters are compared to the ones in the literature for the same device specifications. Moreover, a SAW transducer is modeled for a specific device length from the extracted parameters.

Keywords: Finite element analysis (FEA), Surface acoustic wave (SAW) devices, Bulk acoustic wave (BAW) devices, Interdigital transducer (IDT), Coupling of modes analysis (COM), P-matrix model, Periodic boundary conditions (PBC).

1 Introduction

SAW devices have expanded into a multitude of products and applications in fields as diverse as microelectromechanical systems (MEMS), telecommunications, chemical sensing, and biotechnology [1, 2]. Precise characterization of SAW propagation parameters based on the device geometry and material characteristics is crucial for designing a SAW device. This is commonly performed by manufacturing a test structure, and then extract the needed parameters from the measurements. Such approach is both time consuming and expensive as each device optimisation would require fabricating a test structure. On the other hand, precise numerical methods, mostly BEM/FEM analysis methods have been developed to optimize the design process [3, 4, 5]. In FEM/BEM models the finite elements are used to account for the electrode shapes and the substrate is modelled as boundary elements. This is carried out by replacing the differential equations in the piezoelectric substrate by an integral equation at the boundary using Green's functions. Even though this results in a reduced computational time, the effects of mechanical perturbation, piezoelectric perturbation and energy storage caused by non-radiating bulk waves are not taken into consideration [6].

Considering the dramatic increase in computer performance, available at lower costs, switching from FEM/BEM analysis to finite element modelling (FEM) appears to be a logical choice, where the device is modelled by considering all the partial differential equations. In this paper FEM is used to model a periodic SAW structure to obtain the eigenmodes and harmonic admittance. However, it is important to keep using approximate analytical models like coupling of modes analysis or P-matrix models in parallel, both to understand the basic physical behaviour and to validate the results obtained from finite element modelling. This approach is taken in this paper where the parameters of the periodic structures are extracted from finite element analysis and the simulation results are compared with the analytical model results.

In this paper, in Section 2, we discuss briefly the COM analysis and P-matrix model and highlight the parameters needed in this modelling approach. Then, in Section 3, we use FEM to simulate a periodic structure and identify the SAW eignmodes and obtain the admittance curve. In Section 4, we discuss how the needed parameters are extracted and used in a P-matrix model to model a SAW transducer. Section 4, presents extracted parameters and compares parameters obtained from modelling with measured results in the literature.

2 COM and P-matrix Models

2.1 COM Analysis

Various numerical approximation and simulation techniques are available for the modelling and analysis of SAW devices. Coupling-of-modes (COM) is an appropriate modelling approach where the excitation, propagation and scattering of surface acoustic waves is considered. The COM analysis is based on the Bragg condition, which states that the coupling between the incident and the reflected wave is strong if the

period of the grating, p, is equal or close to half of the wavelength, λ, i.e $\lambda = 2p$. These waves form a stopband by interfering constructively and destructively at two discrete frequencies, where the propagation into the medium is minimum. Only the incident wave and a reflecting wave may be considered in a stopband resulting in a coupling of modes approximation as they have significant amplitudes compared to other harmonics.

The are two ways of deriving the COM equations. First is the algebraic approach where a few hundred harmonics are considered and solved using numerical simulations. We use this approach for modelling the period SAW structures using FEM to derive the COM parameters in this paper. The other approach is the differential method where the truncated algebraic expressions are transformed into linear differential equations and solved. This approach can be easily extended to non-uniform finite structures as the amplitude changes of a very limited number of interacting waves is considered. The derived parameters from the FEM along with this differential approach can be used to model the various SAW components.

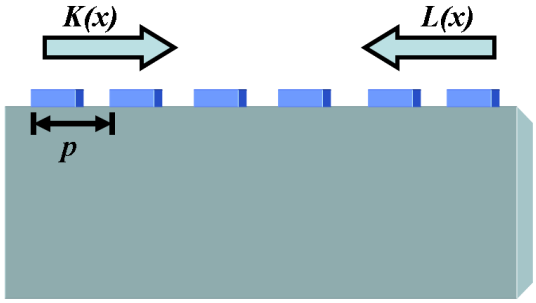

Figure 1: SAW transducer with counter propagating modes.

As shown in Fig. 1 if $K(x)$ and $L(x)$ represent the counter propagating modes in the positive and negative x direction of the structure and $I(x)$ the current caused by the induced charges in the electrodes when the transducer is driven by a Voltage V. Then the first order differential equations derived from the COM model are [7, 8]:

$$\frac{\mathrm{d}K(x)}{\mathrm{d}x} = -j\delta K(x) + j\kappa L(x) + j\alpha V, \quad (1)$$

$$\frac{\mathrm{d}L(x)}{\mathrm{d}x} = -j\kappa^* K(x) + j\delta L(x) - j\alpha^* V, \quad (2)$$

$$\frac{\mathrm{d}I(x)}{\mathrm{d}x} = -2j\alpha^* K(x) - 2j\alpha L(x) + j\omega C V. \quad (3)$$

Where j is the imaginary term and δ is the detuning parameter given by

$$\delta = \frac{2\pi(f - f_0)}{\nu} - j\gamma.$$

The centre frequency f_0 is given by $f_0 = V/2p$, where p is the period of the metal grating. Even though j is present in all the terms of Eqn. (1) - (3) the detuning parameter ensures that they have a real and imaginary part.

In the above equations the independent parameters κ, α, ν, γ and C are reflectivity due to perturbations, transduction coefficient, SAW velocity, attenuation, and capacitance per unit length, respectively. The asterisk denotes the complex conjugate.

The COM parameters are constant for uniform SAW structures hence the general solution for the COM equations (Eqn. (1) - (3)) can be taken as the sum of homogeneous and particular solutions. The homogeneous solution corresponds to the shorted-grated eigenmodes and the particular solution corresponds to the excited field. By excluding the excitation term, i.e by shorting the transducer, the homogeneous solution is obtained. The lower and upper frequencies (f_{M-}&f_{M+}) of the stopband can be obtained by neglecting the attenuation parameter γ [7],

$$f_{M-} = f_0(1 - \frac{|\kappa|p}{\pi}) \quad (4)$$

$$f_{M+} = f_0(1 + \frac{|\kappa|p}{\pi}). \quad (5)$$

In our work the stop band edge frequencies are determined by using modal analysis in the FEM as will be shown in the latter section.

The particular solution is the excited field caused by the drive voltage V applied to the transducer. The amplitude of the excited field is expressed as

$$\begin{pmatrix} K_E \\ L_E \end{pmatrix} = \frac{1}{\delta^2 - |\kappa|^2} \begin{pmatrix} \delta\alpha + \kappa\alpha^* \\ \delta\alpha^* + \kappa^*\alpha \end{pmatrix} V. \quad (6)$$

The amplitudes interfere constructively at one edge of the stopband causing resonance and interfere destructively at the other edge according to the sign of κ. The values of κ and α are real for symmetric structures.

2.2 P-matrix Model

In the design of complex devices the need might arise to use individual electrodes with varying properties, which renders the COM model ineffective. In such structures P-matrix model is an efficient modelling technique where the linear COM equations for each component are expressed as the elements of a matrix called P-matrix. The total response of the device can be determined by the cascading the P-matrices of all the individual components. These cascading techniques and matrix elements are explained in detail in [7, 9].

One of the important elements of the P-matrix is the admittance (P_A), which depicts the electrical behaviour of a uniform bidirectional structure (IDT or a reflector) by relating the current I in the structure to the voltage V and given by [7]

$$P_A = P_A^M + P_A^E. \quad (7)$$

Here, P_A^M is the homogeneous component of the admittance determined by the eigenmodes,

$$P_A^M = -\frac{4\alpha^2(\delta+\kappa)}{n^3} \times \frac{(\delta+\kappa)(1-\cos(nL)) - jn\sin(nL)}{n\cos(nL) + j\delta\sin(nL)}, \quad (8)$$

where L is the length of the device and n is the slowly-varying wavenumber of the eigenmode.

Here, P_A^E is the particular solution component of the admittance caused by the excited field.

$$P_A^E = -j(\frac{4\alpha^2}{\delta-\kappa}L - \omega LC). \quad (9)$$

The P_A^E component dominates the admittance for long structures. These responses are analysed by using harmonic analysis explained in the next section and the admittance curves obtained from the FEA and the P-matrix model are compared.

3 Finite Element Modeling(FEM)

Field theory is the most appropriate theory for the design of SAW devices as it involves the resolution of all the partial differential equations for a given excitation. The Finite element model (FEM) is the most appropriate numerical representation of field theory where the piezoelectric behaviour of the SAW devices can be discretized and numerically solved [10]. With the availability of software package's with large node handling capability and increase in computing performance and memory capacity, switching to a direct FEM for numerical simulation of SAW devices appears to be efficient and straightforward. In the following subsection we will discuss the boundary conditions for periodic structures and the simulations using ANSYS.

3.1 Periodic Boundary Conditions

As the standing waves are spatially periodic in SAW and BAW devices with the same grating shape and substrate it might suffice to simulation just a periodic substructure of the device to reduce the complexity and size of the numerical model. With the use of Periodic Boundary Conditions (PBCs) each mode that can be excited within the periodic structure can be modelled. This analysis of a periodic substructure yields the frequency response and other design characteristics of the whole structure.

One wavelength or even a half wavelength of the device is enough to model the standing wave of the whole structure. As the periodic structure is part of the parent structure, the displacement and electric potential at both the left and right periodic boundaries are made equal. Due to large electrode apertures and predominantly lateral propagation of the surface acoustic waves, a plain strain condition is assumed to reduce the model to a 2D model [11].

3.2 Simulation Results

The simulation of a periodic array which involves solving the system of coupled partial differential equations governing the mechanical and electric fields, in a geometry consisting of the semi-infinite piezoelectric crystal and the periodic electrode array was carried out using ANSYS.

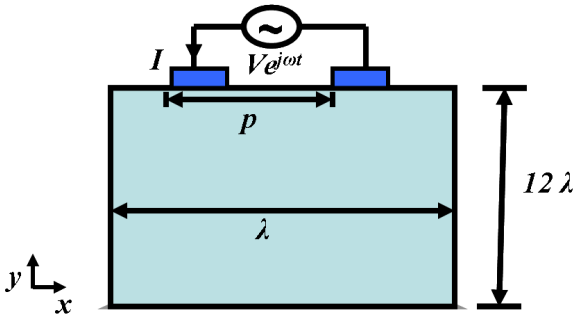

Figure 2: Periodic structure.

For this purpose we consider a periodic structure, as shown in Fig. 2, having a 128° YX-cut $LiNbO_3$ piezoelectric substrate of length 1λ (λ = 4 μm), two Aluminium electrodes with a metallization ratio (MR) of 0.4, and an electrode thickness (h/λ) of 3%. The material properties of the 12λ thick substrate were obtained from [12]. The PBC's are applied to the geometry as explained before and the results of the modal analysis and the harmonic analysis are presented in the following subsections.

3.2.1 Modal Analysis

The homogeneous solution of the differential equations involved in the FEM can be calculated using modal analysis so as to observe the eigenmodes propagating in the structure. The electrodes are shorted for this case and no external drive voltage is applied. By studying the mode shapes of the periodic structures it can be seen that the surface acoustic modes are confined to the top surface. They can be identified and differentiated from the bulk acoustic wave modes, where the displacement and the potential occur in the bulk of the structure.

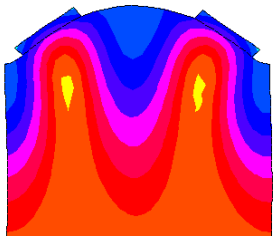

Figure 3: Symmetric SAW mode (f_{M-}) at 907.4 MHz.

Two SAW modes were observed at frequencies of 907.4 MHz and 915.3 MHz for the periodic structure as shown in the Figs. 3 and 4. The differences in

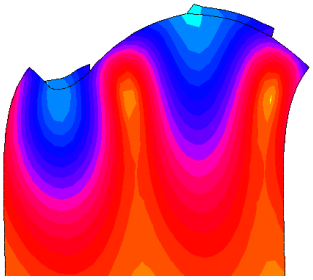

Figure 4: Anti-symmetric SAW mode (f_{M+}) at 915.3 MHz.

the deformation of the IDT's in both the modes can be used to identify the symmetric (f_{M-}) and anti-symmetric mode frequencies (f_{M+}) as explained in [11, 12]. The IDT of the anti-symmetric SAW mode vibrates symmetrically about its centreline. The anti-symmetric SAW mode has a slightly higher frequency than the symmetric SAW mode as that type of vibration requires more strain energy. So from the SAW modal deformation in the Figs. 3 and 4, f_{M-} is 907.4 MHz and f_{M+} is 915.32 MHz.

3.2.2 Harmonic Analysis

The particular solution corresponding to the excited field of the differential equations can be obtained by using harmonic analysis. A drive voltage is applied across the electrodes and a steady state response is examined around the stopband edge frequencies, obtained from the modal analysis. All the nodes of the electrodes are coupled to keep the electric potential on the nodes constant. The displacement contour of the periodic structure is shown in the Fig. 5 when driven by a 2 V_{pp} voltage at a frequency of f_{M+}. It can be observed that the displacement is confined to the top surface of the structure with a maximum value of 0.644 nm close to the electrodes.

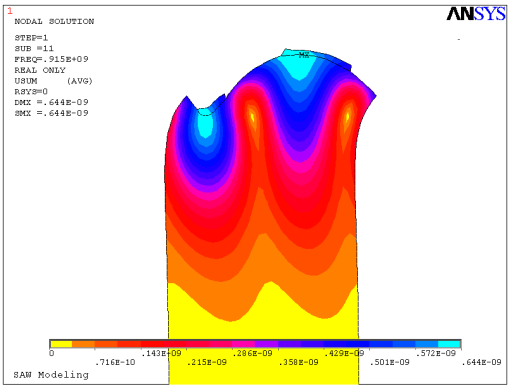

Figure 5: Displacement Contour.

The harmonic admittance which characterises the electrical behaviour of the SAW device can be determined from the complete charge distribution of the electrodes. If q is the complex charge of the electrode then the admittance Y is given by [13],

$$Y = j\frac{q\omega}{V}, \tag{10}$$

where ω is the angular frequency.

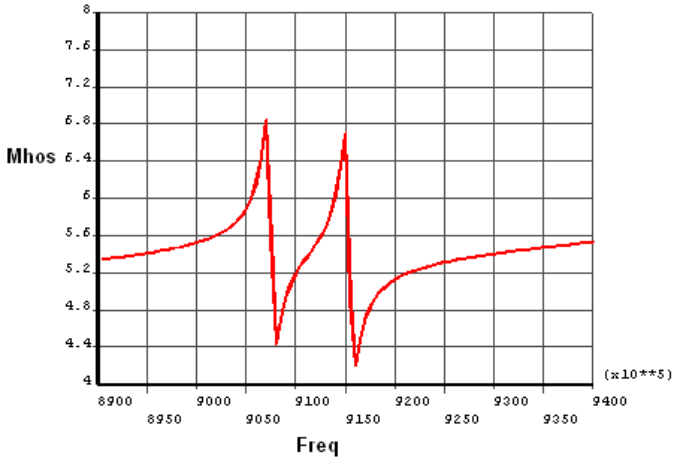

Figure 6: FEM Admittance magnitude curve.

The admittance magnitude curve obtained from the FEM is depicted in the Fig. 6. It can be observed that the resonant peaks in the admittance curve coincide exactly with the stopband edge frequencies obtained from the modal analysis.

4 Parameter Extraction

The parameters in the COM equations (Eqn. (1) - (3)) are influenced by the material properties of the structures, crystal cut, shape of the electrodes, metallization ratio and aperture. These parameters can be normalized to the periodicity and aperture A of the structure, as shown in Table 1, so that they remain scale-invariant constants.

Table 1: Normalized COM Parameters [5]

Parameter	Symbol
Velocity	ν
Reflectivity	$\kappa_p = \kappa\lambda_0$
Transduction coefficient	$\alpha_p = \alpha\lambda_0$
Normalised transduction	$\alpha_n = \alpha_p/\sqrt{\frac{A}{\lambda_0}}$
Attenuation	$\gamma_p = \gamma\lambda_0$
Capacitance	$C_p = C\lambda_0$
Normalized capacitance	$C_n = C_p/A$

By computing the projection of FEM analysis onto the set of the field distributions predicted by the coupled-mode theory, we can derive the parameters corresponding to COM equations [6]. Hence Eqns (4) and (5) can be rewritten as

$$\nu = p(f_{M-} + f_{M+}) \tag{11}$$

$$\kappa_p = \pi\frac{f_{M+} - f_{M-}}{f_{M+} + f_{M-}}. \tag{12}$$

The obtained short grated stopband edge frequencies (f_{M+} & f_{M-}) from the modal analysis can be substituted in Eqn (11) and (12) to extract the velocity and reflectivity parameters for one period of the structure. The sign of the reflectivity κ_p determines the location of the symmetric and anti-symmetric SAW modes.

The admittance curve obtained from the harmonic analysis in the previous section corresponds to the particular solution in Eqn (6) caused by the excited field. All the other COM parameters can be determined from the characteristics of the curve, which is a direct representation of the electrical admittance of the experimental structure.

The fitting technique used by [5] to determine the parameters of Green's function model is utilised to extract the parameters from the FEA computed admittance curve. The equations corresponding to this technique are given below.

The P_A^E component in Eqn (9) dominates the admittance for the infinitely long structures considered here. So the admittance for a periodic structure can be expressed as

$$Y = -j\frac{4\alpha^2\lambda_0}{\delta+\kappa}L + j\omega C_p. \tag{13}$$

Let Y_r and Y_i denote the real and imaginary parts of the admittance in Fig. 7, respectively. The resonant frequency f_R, which is frequency at the peak of the real admittance $Y_{r\max}$ is given by

$$f_R = f_0(1 - \frac{\kappa_p}{2\pi}). \tag{14}$$

and the peak of the real admittance part is

$$Y_{r\max} \equiv Y_R(f_R) = \frac{4{\alpha_p}^2}{\gamma_p}. \tag{15}$$

If Δf is the width of the real admittance peak at $Y_R = Y_{r\max}/2$ then

$$\Delta f = \frac{f_0\gamma_p}{\pi}. \tag{16}$$

All the information contained in the curve is described by the quantities in the above equations, from where the transduction coefficient α_p and the attenuation γ_p can be obtained.
The real and imaginary parts of the admittance can be expressed as:

$$Y_r(f) = \frac{Y_{r\max}}{4Q^2(f/f_R-1)^2+1}, \tag{17}$$

and

$$Y_i(f) = -Y_{r\max}\frac{2Q(f/f_R-1)}{4Q^2(f/f_R-1)^2+1} + 2\pi f C_p. \tag{18}$$

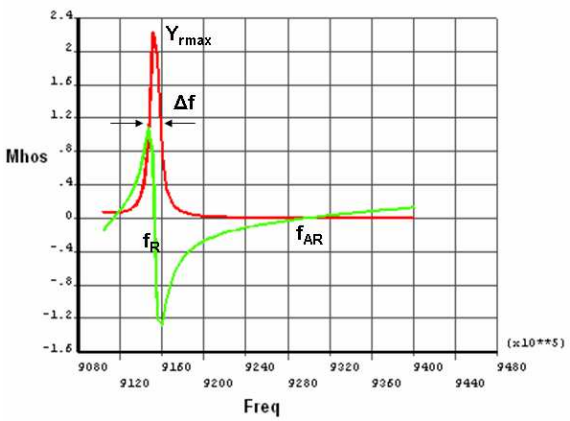

Figure 7: FEM admittance curve with real and imaginary parts at f_{M+} mode frequency.

As the imaginary part of the admittance crosses zero at the antiresonance frequency f_{AR} then Eqn (18) can be equated to zero at that frequency to find C_p

$$C_p = \frac{Y_{r\max}}{2\pi f_{AR}} \times \frac{2Q(f_{AR}/f_R-1)}{4Q^2(f_{AR}/f_R-1)^2+1}$$

where $Q = f_R/\Delta f$ is the quality factor.

All the COM parameters can be extracted by applying the above equations to the observed quantities in the admittance curve of Fig. 7. The extracted parameters for SAW on 128° Y-cut X-propagating $LiNbO_3$ with rectangular aluminium for a metallisation ratio (MR) of 0.4 and electrode thickness(h) of 3% are presented in the Table 2 and compared with those in the literature [7] calculated by using FEM/BEM analysis. The differences in the values of velocity can be attributed to mass loading effect and small SAW propagation in to the substrate. As there is no attenuation on the free surface in numerical simulations a small attenuation was introduced externally, which does not effect other parameters. The parameters α_n and C_n could not be compared with the one's in the literature because of the differences in the aperture length.

Table 2: COM Parameters for 128° YX-cut $LiNbO_3$ with MR of 0.4 and h of 3%

Parameter	Current work	[7]	units
ν	3828	3885	m/s
κ_p	-0.024	-0.026	
α_n	41.5×10^{-5}		$\Omega^{-1/2}$
C_n	115.6×10^{-5}		pF/μm

The extracted parameters are substituted in Eqn. (9) for a structure length of 150λ to get the COM/P-matrix admittance curve as shown in Fig. 8. The location of the resonant peak at center frequency is in excellent agreement with the FEM simulations. These simulation results and the extracted parameters from the results match well with the ones in the literature

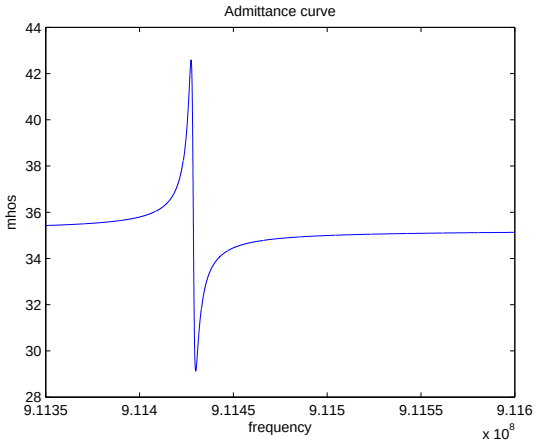

Figure 8: Admittance curve from P-matrix using the extracted parameters.

for the same specifications. The simulation results in the literature were in turn validated with physical SAW devices.The next step would be to validate the results using experimental test devices, which the authors would like to consider as future work.

5 Conclusion

In this paper we demonstrated the use of finite element approach to model a periodic SAW structure where the complete set of partial differential equations is considered to include all the second order effects. From the FEM simulations, the eignmodes and the admittance curve for a periodic structure are obtained. Then COM/P-matrix parameters are extracted from the simulation results using a fitting technique. These parameters are then used in obtaining the admittance element of the P-matrix model for a specific SAW transducer length. By extracting the needed parameters from the admittance curve of a periodic substructure we demonstrated that the admittance curve for a structure can be found without the need to perform FEM for the whole device length, which can be computationally challenging for large device length.

6 Acknowledgements

The authors would like to thank the Australian Research Council (ARC) and the School of Electrical and Electronics Engineering (University of Adelaide) for the funding and support for the project.

7 References

[1] A. Mamishev, K. Sundara-Rajan, F. Yang, Y. Du and M. Zahn, "Interdigital Sensors and Transducers," *Proceedings of the IEEE*, 92(5), pp 808–845 (2004).

[2] I. Pitz, L. Hall, H. Hansen, V. Varadan, C. Bertram, S. Maddocks, S. Enderling, S. Al-Sarawi and D. Abbott, "Trade-Offs for Wireless Transcutaneous RF Communication in Biotelemetric Applications," in *Proc. of SPIE Symposium on Biomedical Applications of Micro- and Nanoengineering*, volume 4937, pp 307–18 (2002).

[3] P. Ventura, J. Hode and M. Solal, "A new efficient combined FEM and periodic Green's function formalism for the analysis of periodic SAW structures," in *Proc. of IEEE Ultrasonics Symposium*, pp 263–268 (1995).

[4] P. Ventura, J. Hode, M. Solal, J. Desbois and J. Ribbe, "Numerical methods for SAW propagation characterization," in *Proc. of IEEE Ultrasonics Symposium*, pp 175–186 (1998).

[5] J. Koskela, V. Plessky and M. Salomaa, "SAW/LSAW COM parameter extraction from computer experiments with harmonic admittance of a periodic array of electrodes," *IEEE Trans. on Ultrasonics, Ferroelectrics, and Frequency Control*, 46(4) (1999).

[6] K. Hasegawa, K. Inagawa and M. Koshiba, "Extraction of all coefficients of coupled-mode equations for natural, single phase by hybrid finite element method," *IEEE Trans. on Ultrasonics, Ferroelectrics, and Frequency Control*, 48(5) (2001).

[7] V. Plessky and J. Koskela, "Coupling-of-Modes Analysis of SAW Devices," *International Journal of High Speed Electronics and Systems*, 10(4), pp 867–947 (2000).

[8] C. K. Campbell, *Surface Acoustic Wave Devices for Mobile and Wireless Communications*, Academic Press: Boston (1998).

[9] D. Morgan, "Cascading formulas for identical transducer P-matrices," *IEEE Trans. on Ultrasonics, Ferroelectrics, and Frequency Control*, 43(5) (1996).

[10] M. Hofer, N. Finger, G. Kovacs, J. Schölmer, U. Langer and R. Lerch, "Finite Element Simulation of Bulk and Surface Acoustic Wave (SAW) Interaction in SAW Devices," in *Proc. of IEEE Ultrasonics Symposium*, pp 53–56 (2002).

[11] Y. Yong, "Analysis of periodic structures for baw and saw resonators," in *Proc. of IEEE Ultrasonics Symposium*, pp 781–790 (2001).

[12] T. Kannan, *Finite Element Analysis of Surface Acoustic Wave Resonators*, Master's thesis, University of Saskatchewan (2006).

[13] M. Hofer, N. Finger, G. Kovacs, J. Schölmer, S. Zaglmayr, U. Langer and R. Lerch, "Finite-Element Simulation of Wave Propagation in Periodic Piezoelectric SAW Structures," *IEEE Trans. on Ultrasonics, Ferroelectrics, and Frequency Control*, 53(6) (2006).